ALMA MATER STUDIORUM · UNIVERSITÀ DI BOLOGNA

Scuola di Scienze
Dipartimento di Fisica e Astronomia

Corso di Laurea in Fisica

Ageing effects on Optoelectronic Characterization of PEA single crystals

Relatore:
Prof.ssa Beatrice Fraboni

Correlatore:
Dott. Andrea Ciavatti

Presentata da:
Mariagrazia Moliterni

ANNO ACCADEMICO
2023/2024

Abstract

Le Perovskiti rappresentano una larga classe di materiali che sono descritti attraverso la formula ABX_3 , in cui A rappresenta il catione organico, B il catione inorganico e X l'anione alogenuro. Essendo facilmente producibili in un ambiente controllato e mostrando ottime qualità optoelettroniche, come Responsivity, External Quantum Efficiency e Detectivity ,le Perovskiti si prestano a vasti campi di applicazione, dalle celle fotovoltaiche ai rilevatori di particelle. Un aspetto cruciale della loro versatilità è però l'influenza dell'ambiente esterno: le Perovskiti tendono infatti a deteriorarsi molto in un ambiente non controllato e sono perciò soggette a un veloce degrado nel tempo.

In questo lavoro di tesi sono stati presi in considerazione tre campioni con differenti gradi di difettosità note al fine di studiarne l'influenza sulle proprietà optoelettroniche dei rilevatori considerati. È stata eseguita una analisi delle loro caratteristiche di tensione e corrente per calcolare i parametri fisici che classificano i detector presenti sul mercato, nonché per confrontare gli stessi con i dati presi due anni fa durante un precedete studio di tesi.

Si è provato, inoltre, ad eseguire una analisi dei transienti di corrente a seguito di un impulso luminoso a frequenza costante prodotto da led e a diversi step di temperature per poter meglio classificare le difettosità e, ancora una volta, confrontarle con quelle già eseguite in passato. Queste ultime analisi, però, seppure in grado di rilevare i transienti di corrente, non hanno prodotto informazioni aggiuntive poiché non si è riuscito a rilevare segnali significativi per l'analisi. Tali considerazioni sono state quindi escluse dalle conclusioni dedotte a seguito dello studio.

Da questo lavoro è emersa la conferma che le difettosità incidono sulle proprietà optoelettroniche dei rilevatori analizzati anche se il degrado di tali proprietà nel tempo non lo si può con certezza imputare alle condizioni con cui il materiale viene conservato o alle difettosità presenti in esso.

Contents

Introduction

Nowadays semiconductor devices play a crucial role in many daily applications, from renewable energy to sensing, lighting, telecommunications, and consumer electronics. Currently, the most commonly employed semiconductors are inorganic materials such as silicon and germanium. These materials provide stable and reliable performance, and their high cost of production has decreased over the years, thanks to the economy of scale. Nonetheless, they are still affected by some limitations. One of them is their limited mechanical flexibility: semiconductors are rigid and brittle, and therefore unsuitable for being used in flexible electronics to produce, for instance, roll-up displays and wearable devices. Another relevant limitation is their high cost of production; in fact, despite the decrease in their manufacturing cost over the years, the processes needed for inorganic semiconductor production are inherently expensive in terms of energy use. In particular, they require high temperatures and high vacuum, which inevitably increase production cost.

These limitations have pushed research towards the study of new semiconducting materials: organic semiconductors have been found to provide a valid alternative to those. For this reason researchers are focussing on hybrid metal halide perovskites (MHPs), which demonstrate outstanding performances in all sorts of optoelectronic devices and applications. These materials combine the simple and low-cost fabrication process of organic semiconductors, while maintaining remarkable optoelectronic characteristics such as tuneable band gap, high adsorption coefficient and great mobility lifetime.

Hybrid Organic-Inorganic Halide Perovskites (HOIPs) include a large class of materials described with the general formula ABX_3, where: A is an organic cation, B an inorganic cation and X an halide anion. A subclass of these materials, the so-called two-dimensional (2D) layered HOIPs, have emerged as potential alternatives to traditional 3D ones for enhancing the stability and increasing the performance of perovskite devices, with particular regard in the area of ionizing radiation detectors, where these materials have reached truly remarkable milestones.

On the other side, the main problem with HOIPs is their stability: HOIPs are, in fact, extremely sensitive to environmental conditions

and humidity, since in this conditions they can degrade within days or even hours.

In this work, deep states in Perovskites semiconductors have been studied through means of Photo-Induced Current Transient Spectroscopy (PICTS), a highly sensitive spectroscopic technique capable of detecting the presence of deep states in highly resistive ohmic materials and characterizing their activation energy, capture cross section and, under stringent conditions, the concentration of these states. Another step has been done in characterization, by studying the effects of ageing on PEA_2PbBr_4 samples perovskites, which, in Hofstetter et al. [1] , proved to be one of the most stable materials to degradation among 2D perovskites.

1. 2D Hybrid Perovskites

1.1. Defect states in a crystal lattice

A crystal is an ordered structure that occurs from the intrinsic nature of the constituent particles to form symmetric patterns that repeat themselves along the principal directions of three dimensional space in matter. The differences between a mathematical conceptualization of a crystalline material and a real crystal is that the latter has finite dimensions and defects in its structure that affect its physical behaviour of condensed matter: let's consider that when the dimensions of the material fall within ordinary everyday dimensions, the edge of the crystal contains around 10^8 atoms and the ratio of atoms in the bulk of the surface turns out to be about $1/10^8$. What makes a material "real" and gives it many of the properties that do not naturally emerge from the band structure are precisely those conditions that interrupt the periodicity of the crystal structure. These features are commonly referred to as "crystalline defects" and can be divided into point, linear, surface and bulk defects. It is also easily demonstrated, for example, from classical statistical mechanics, that a crystalline solid cannot exist in a thermodynamically stable configuration without a minimum amount of crystalline defects [2]. The word "defect" is actually a misleading term: it is something that usually needs to be removed. Here, actually, "defects" play a fundamental role in solid-state physics, and it is through the study, knowledge and engineering of them that contemporary technology thrives. In solid state physics, the study of defects plays such an important role that physicists define micro- and nanostructured materials as "the set of crystalline defects that characterize the properties of the micro- or nano-structure". Defects, indeed, characterize many properties of solids such as the hardness of steel, thermal properties that make certain materials highly efficient insulators, but also that make rubies red and certain gems green. Through the knowledge and control of these crystalline defects it is possible to control the behaviour of a material to have ever more efficient LEDs and solar cells for example, more powerful lasers and faster transistors. Defects can be "punctual", like vacancies that respect charge neutrality (namely the Frenkel-type or Schottky-type defects) or

vacancies that are occupied by electrons, impurity atoms that replace others in the material hosting these impurities or interstitials . It may also happen that impurities atoms are deliberately inserted into the material: this is a procedure called *doping*, and represents a fundamental technique for modulating the opto-electronic properties of a semiconductor. Punctual defects relevant in the study of radiation detector properties are those that introduce charge-carrier-occupiable energy states within the energy gap of the semiconductor used as a detector of radiation. These states can be grouped into two categories: *shallow state*, when the energy state due to the crystalline defect is near the valence band or the conduction band, and *deep state* that act as recombination centers for charge carriers, and are all the more efficient the closer they are to the Fermi level. For this purpose we define the activation energy (E_a) as the difference in energy content between atoms or molecules in an activated or transition-state configuration and the corresponding atoms and molecules in their initial configuration. [3]

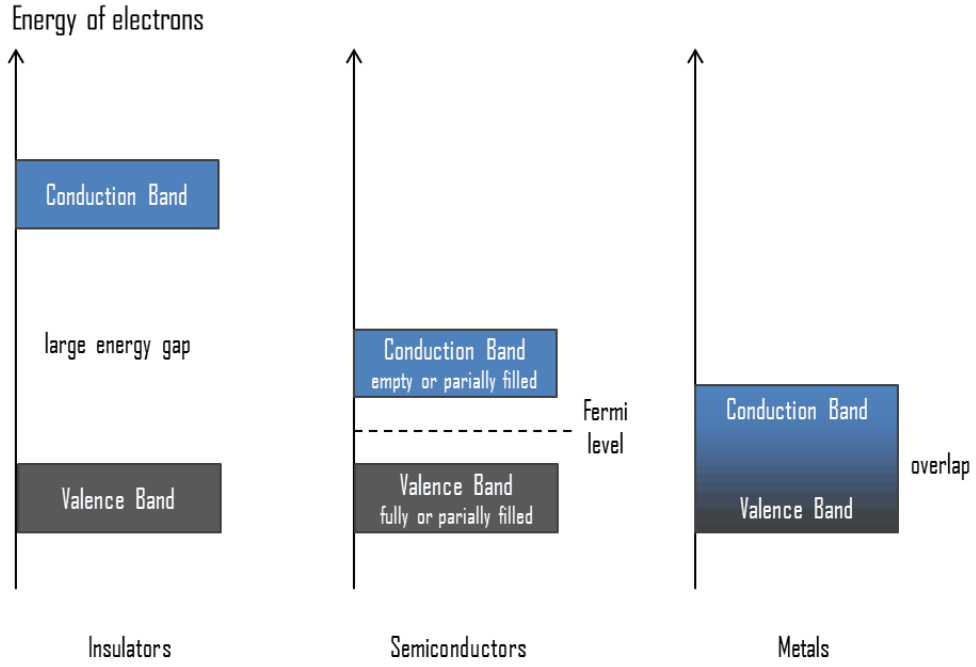

Figure 1 Explanation of the differences: Insulators, Semiconductors and Metals

For conventional semiconductors like Si and GaAs, the threshold activation energy to distinguish between deep and shallow states is typically considered as twice the thermal energy at room temperature, i.e. $E_a \sim 0.05eV \sim 2k_bT$. This means that shallow states are thermally ionized at room temperature, so they act as dopants.

On the contrary, deep states are not ionized at room temperature, and for this reason are often referred to as trap states.
When a high energy photon reaches the sensitive part of a detector, a cascade of charge carriers
occurs. These charge carriers will become a measurable current if and only if they can reach the electrodes. Trap states prevent this process, limiting the efficiency of the detector. There is no simple model to describe the effects of deep defects on crystal properties as we have seen for shallow states. What we do have, however, is a statistical approach developed complementarily and independently in 1952 by W. Schottky and W.T. Read [4] and R.N Hall [5]and takes the name of SRH model, from the initials of the three physicists.

1.1.1 SRH model for deep states

A good way to describe what happen in deep states is outlined in *Figure 2*, where a trap state with energy E_t falls within the band gap of a semiconductor, marked between Valence band with energy E_v and Conduction band with energy E_c :

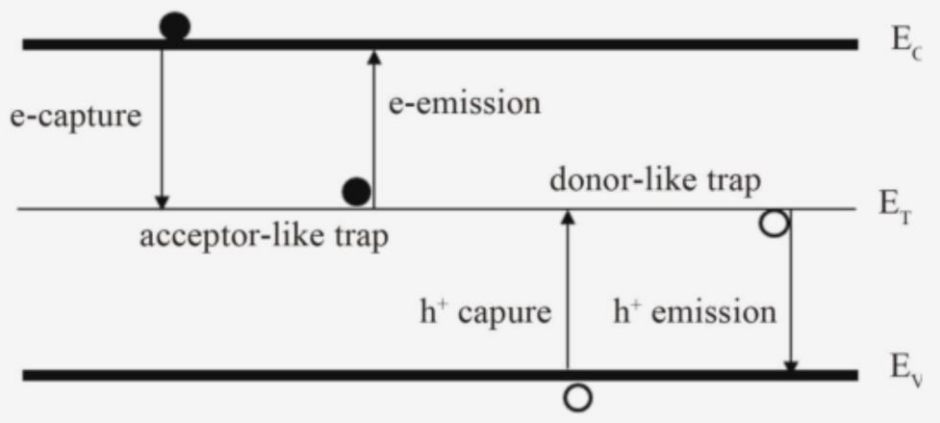

Figure 2 A defect introduces an energy level E_t into the band gap, then four physical processes can occur: capture/emission of an electron by the trap, capture/emission of a hole by the trap

These processes can be represented mathematically through the following four equations:

$C_e = V_{thn}\sigma_n n N_t(1 - f_t)$
$E_e = e_n f_t N_t$
$C_p = V_{thp}\sigma_p p N_t f_t$
$E_p = e_p(f_t - 1)N_t$,

where $V_{thn}(p)$ is the electron (hole) thermal velocity, $\sigma_n(p)$ is called capture cross section for electron (hole), $f_t = 1/(1 + \exp(E_t - E_f))$ is the Fermi-Dirac statistics for the trap, $e_n(p)$ is the thermal emission rate for electron (hole) by the trap, n(p) is the electron (hole) density and N_t is the trap density with energy E_t. These equations represent the probability of an electron to be captured or emitted by a trap and the probability of an hole to be captured and emitted by a trap, respectively. f_t represents the probability that a trap is occupied by an electron.
Written in this way, it is easy to see that the electron capture rate is directly proportional to the trap density, the electron density, and the probability that the trap is empty (which is equivalent to say that it is occupied by a hole). In contrast, for a hole the capture rate is proportional to the hole density, trap density and the probability that the trap is occupied by an electron. Necessarily, the trapping processes must depend on the thermal velocity of the charge carriers, since by their nature (related to Fermi-Dirac statistics) they are thermally activated phenomena. The capture process is characterized by a capture cross section, σ, analogous to the concept employed in nuclear physics.
From here, with some simple algebra we can extract the general formula for electron (hole) thermal emission rate:

$$e_{n(p)} = V_{thn(p)}\,\sigma_{n(p)} N_{C(V)} \exp\left(\pm \frac{E_T - E_{C(V)}}{K_b T}\right)$$

$N_{C(V)}$ is the electron (hole) density at the edge of the conductance (valence) band.

1.2. Hybrid Organic-Inorganic Perovskites (HOIPS)

Metal-Halide Hybrid Organic-Inorganic Perovskites, commonly abbreviated as HOIPs are a class of ionic materials with crystal structure ABX_3, where A is a monovalent cation, B is a divalent metallic cation, and X is a halogen monovalent anion. Their unit cell is schematically represented in *Figure 3*:

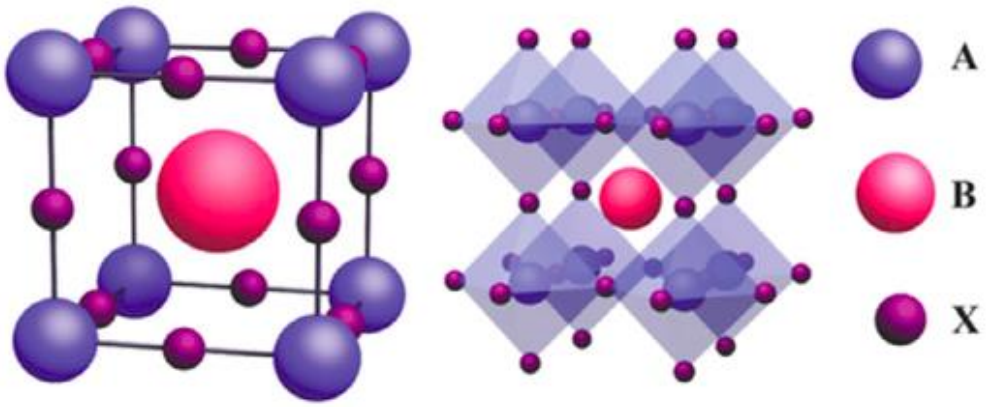

Figure 3 Unit cell of Hybrid Organic-Inorganic cubic perovskite crystal(left). Extended perovskite crystalline structure (right)

HOIPs are crystal structures that can occur with three-, two-, one- or zero dimensional electronic degrees of freedom. The crystal structure is formed by a network of AX_6 octahedra, within which lays a type B cation, which share an X-type anion in the vertices. Eight of these octahedra enclose within the interstitial site, cuboctahedral in shape, an organic molecular cation B. The term hybrid will indicate the presence of organic and inorganic components in the same material. The most common cation in A-site are Pb, Sn and, possibly, other isovalent metals. The anion in X-site is an halide chosen between Cl, Br, I. The contribution from the organic cation only affects the electronic states several eV below the valence band. This indicates a weak interaction between the organic cation and the inorganic ions. However, this does not mean that the organic cation has little impact on the structural, and opto-electronic properties: the choice of the organic cation is essential to determine the crystal structure and phase transitions of the HOIPS. Moreover, changing the organic molecule allows to fine-tune the bandgap and to optimize the absorption of optoelectronic devices. 2D HOIPs are a class of compounds that shared a peculiar crystal structure, in which one or more layers of inorganic material are superimposed on a layer of dielectric organic material. Their electronic structure is similar to a multiple quantum well. This structure gives these materials truly distinctive opto-electronic properties, making them excellent candidates in many technological applications.

1.2.1 Optical properties and critical issue of HOIPS

The importance of HOIPS lays in the fact that these systems can be considered as a natural multiple quantum wells in which the inorganic material acts as a potential well and the insulating organic layers act as potential barriers. The electron confinement occurs over sub-nanometric distances and induces the generation of stable room temperature excitons, with high binding energy and a Bohr radius that extends beyond the boundaries of individual layers. It seems that the stability of the exciton also derive from the organic layer that plays an important role by modulating the dielectric properties of the material. Also, the complex layered structure of 2D perovskites naturally self-assembles during the synthesis process. This structure, combined with the organic properties of the potential barrier, leads to the formation of stable states even at high temperatures. The possibility of being able to modify the variety of the organic molecule, of the metal and of the halogen, means that the band gap of these perovskites can be finely tuned in a wide range that goes from visible to ultraviolet field. Compared to traditional high-temperature-prepared inorganic semiconductors, 2D HOIPs can be prepared by solvent evaporation at room temperature, which creates few defects in crystals. In addition, 2D perovskites have low sensitiveness to defects, and are therefore a good candidate for high performance photodetectors with high reactivity and low dark current. Because of excellent stability and exceptional optoelectronic properties, 2D layered perovskites performed better in photodetectors than their 3D counterparts. The photoluminescence quantum efficiency makes 2D perovskites excellent candidates not only as X and γ ray detectors, but also as active components in photovoltaic cells and white light LEDs. 2D perovskites, also, show great stability with respect to humid environments, to large electric fields, to light, aging, vacuum and ionizing radiation. On the other hand, HOIPs are very unstable materials when exposed to normal environmental conditions and can degrade, losing their optical, mechanical, electrical and morphological characteristics, within days or even hours if exposed to environmental conditions where high humidity, for example, is present. Other factors such as exposure to heat, light, and electric fields also speed degradation [6]. This characteristic makes practical applications of this new family of materials difficult, although many

advances have been made in recent years. Precautions such as encapsulation of the material to protect it from external conditions make it possible to extend its life, although we are still a long way from achieving the stability exhibited by inorganic semiconductors. This is one of the biggest challenge the scientific community is facing regarding HOIPs. So far, there is not a complete understanding regarding the physical factors as the root of this rapid degradation, but some work suggests that it is precisely the low ion activation energy that causes the easy migration of atoms and molecules that reassemble to create compounds that go on to define crystalline defects [7].

2. Materials and Methods

2.1. Samples under analysis: PEA_2PbBr_4

The synthesis of PEA_2PbBr_4 follows a simple slow and controlled evaporation process. Starting from the precursors PEABr and $PbBr_2$ the following stoichiometric formula is obtained:
$2PEABr + PbBr_2 \rightarrow PEA_2PbBr_4$
The precursors are then mixed in the right stoichiometric proportions and dissolved in DMF (N,N-Dimethylformamide). Solutes and solvents are combined to form a 1.3 molar solution (slightly above the supersaturation value of the solute in the solvent), and remains overnight in a closed container inside which they are mixed by a stirrer. Then the solution is passed through special filters and placed in a beaker. The beaker is covered with a waxy film to which four holes with a diameter of about one millimetre are made: this process reduces any impurities that can act as nucleation centres and reduces the evaporation rate.
The driving force of the seeded growth from a solution is the supersaturation state of the solute in the solvent, which can be achieved by solvent evaporation. The success of the synthesis process depends mainly on the speed with which the solution evaporates, which must be as slow as possible. After about three weeks, nucleation phenomena occur which lead to the formation of crystals with an approximately rectangular shape with sides ranging from a few millimetres to about one centimetre. This process can

be defined as a steady-state nucleation growth rate at the crystal surface [8].
In this thesis work three single crystal have been considered, studying their as-grown optoelectronic properties, analysing the data acquired 2 years ago by a previous work and repeating the characterization today, with the aim of studying the effect of ageing after 2 years.
The three samples are named as:
Cr01, Au03, Au04, referring it to the element that result from saturation of the solute in the solvent during the creation process.
With the aim of analyse how defects affect the properties of Perovskites, the Au samples have been contaminated with different portion of water, one mole for Au03 and a ten moles for Au04, while Cr01 is pure without contamination.
In *Figure 4* the three samples are shown under microscope:

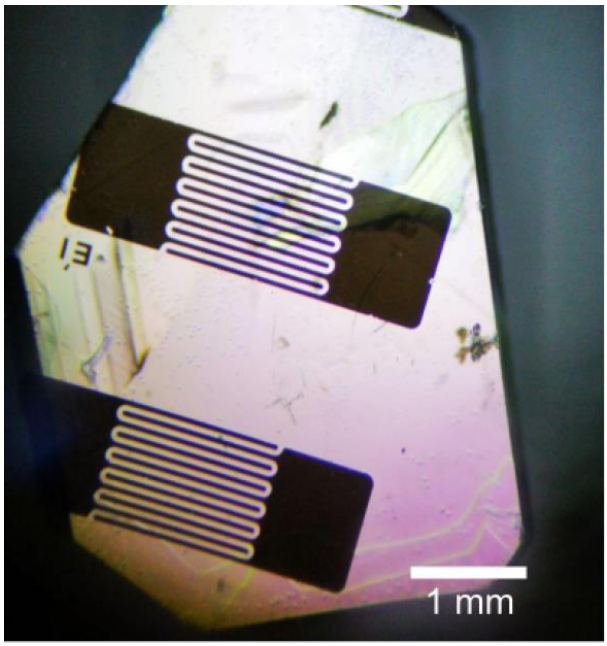

(a)

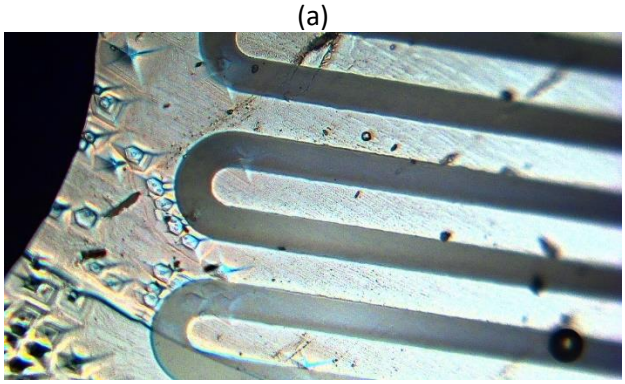

(a2)

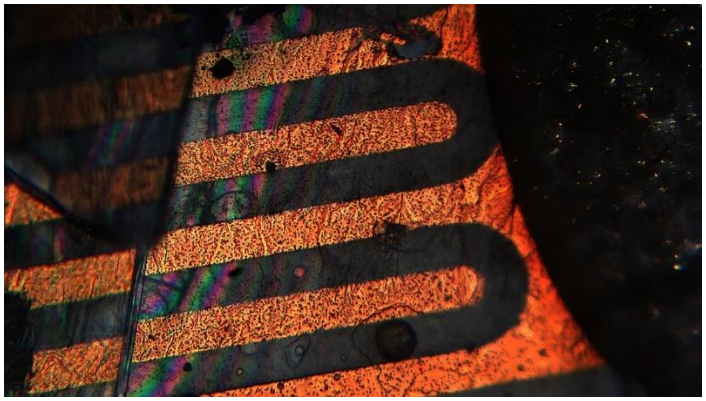

(b)

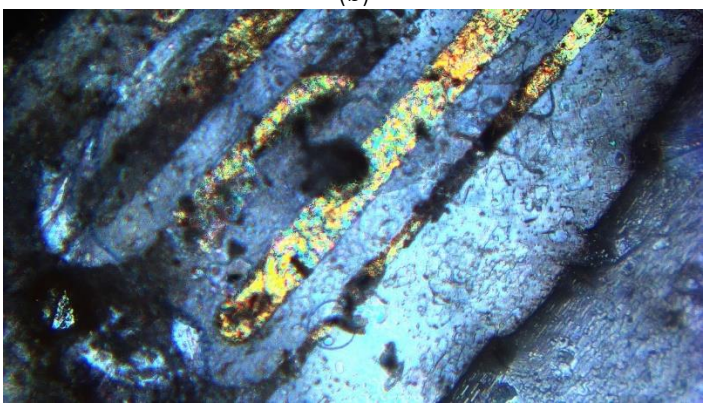

(c)

Figure 4 Samples under microscope: a)Cr01 when fabricated in 2022, a2)Cr01, b)Au03 and c)Au04 in 2024

SAMPLE	ACTIVE AREA	INTERDIGIT	RECEPIT	DEFECTIVENESS
Cr01	1.3 mm^2	40 µm	pure	Defect-free
Au03	1.3 mm^2	40 µm	+1 mol H_2O	Defective
Au04	1.3 mm^2	40 µm	+10 mol H_2O	Highly defective

Table 1 Summary of the samples

2.2. Photo-Induced Current Transient Spectroscopy PICTS

Photo Induced Current Transient Spectroscopy (PICTS) is one of the simplest experimental techniques to trace the band gap of a semiconductor material. It is based on the idea that, in a semiconductor, only the incident radiation with a wavelength less than a critical wavelength is absorbed, promoting an electron from the valence band to the conduction band, thus generating a current. Therefore, taking a source of white light and breaking it down into its fundamental components, it is possible to evaluate the photocurrent as a function of the wavelength. In fact, a PICTS experiment can be summarized with the following two steps:

1) charge carriers are produced through an optical excitation and fill the traps;
2) the optical excitation is switched off and the transient of the electric current is measured, which carries with it information about the thermal emission from the traps.

These two steps are repeated during a temperature scan. The acquired signal is therefore a collection of current transients as a function of temperature. Subsequently, through an elaborate data analysis, it is possible to experimentally access the thermal emission rate e_n (or e_p for hole), and therefore measure the capture cross section, the activation energy and, possibly, the concentration for each trap present in the material. The SRH model tells us that it is possible to access the values of the activation energy and capture cross section of the traps (at least the apparent values) if we know the thermal dependence of the emission rate of the traps and for this purpose, PICTS technique allows us to experimentally find this link with the current transient that occurs when the external radiation is turned off.

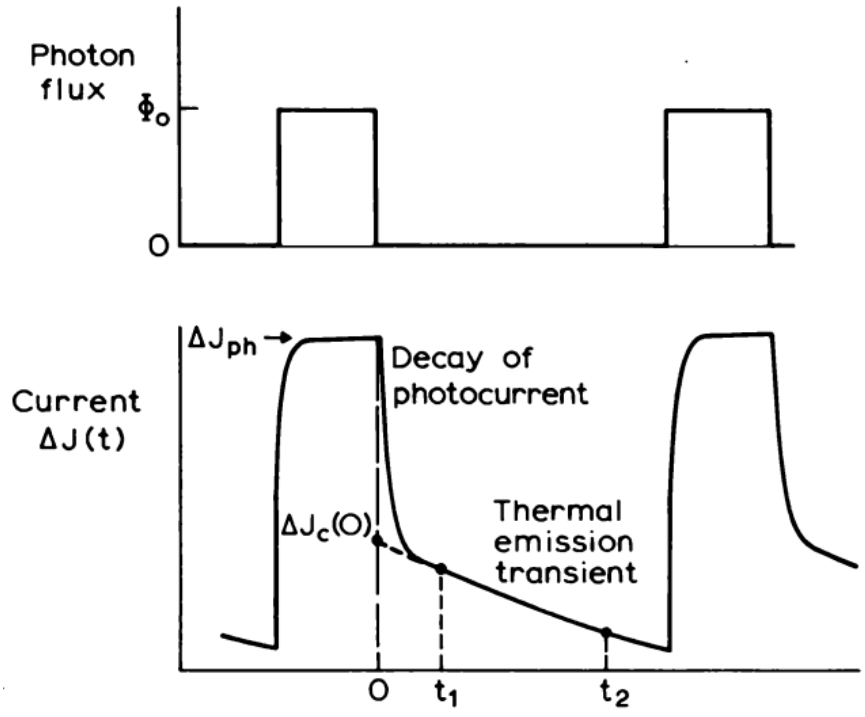

Figure 5 Current response due to the irradiation of a sample with electromagnetic radiation of an appropriate energy: when the external radiation is turned off, the value of the current collapses, but a few moments later there is a thermal transient due to the emptying of the traps [9]

Initially the plateau reached by the photocurrent drops abruptly, but a current transient remains, due to the thermal emission rate of

the traps that are emptying. *Figure 5* schematizes the processes described so far.

2.2.1. The Double-Gate Method and the concept of Rate Window

Now that we have the model that represents the thermal dependence of its characteristic we can build our PICTS signal. The basic idea is similar to many other transient spectroscopy techniques and is based on the "rate windows" concept. The rate window is an arbitrarily chosen time interval from where we measure the difference in the current value.

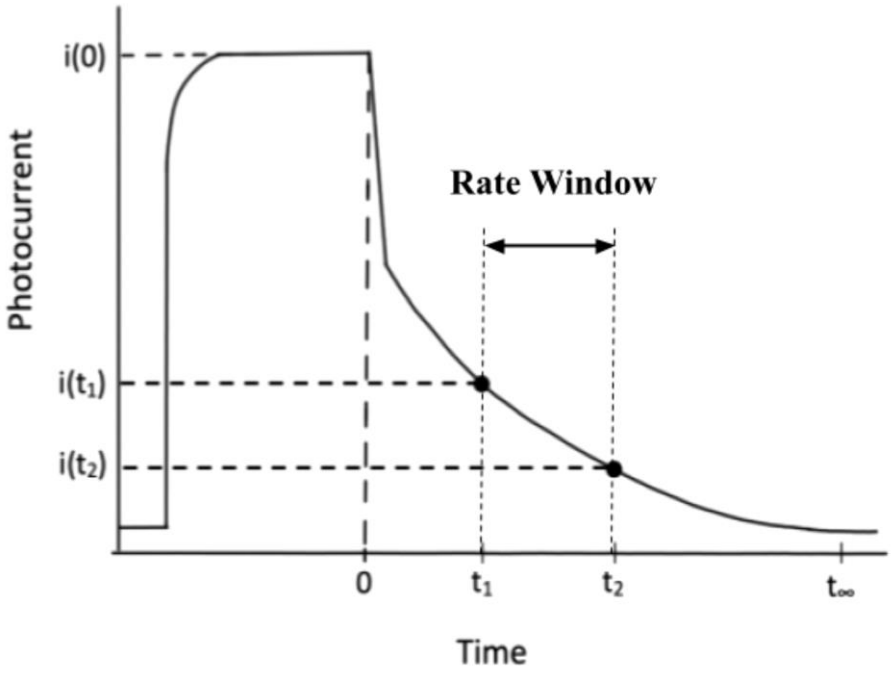

Figure 6 The shape of a photo-induced current transient: t1 and t2 represent two instants of time chosen to measure the PICTS signal. These instants of time are called Rates Window.

Referring to *Figure 6*, the instant t = 0 coincide with the LED turned off. Once the time instant in which the transition to thermal emission occurs has been defined in the electrical transient (we can call this instant t_0), we choose two successive instants $t_1 > t_0$ and $t_2 > t_1$ and express the PICTS signal as the difference in the value of the currents in these two instants:

$$\begin{aligned} \mathrm{S(T;}\ t_1, t_2) &= \mathrm{i}(t_1,) - \mathrm{i}(t_2) \\ &= \frac{Ld}{l}\ \mathrm{q}V\mu\tau n_t(0) e_n (e^{-e_n t_1} - e^{-e_n t_2}) \end{aligned}$$

If there was no thermal emission from the traps, the current difference between the two fixed points would simply be a constant as the decay of the transient would not be perturbed by the emptying of the traps. If a trap is present, instead, we expect the thermal emission to reach a maximum at a certain temperature T_m, and therefore also the difference in the PICTS signal will be characterized by a maximum exactly at the point where the thermal emission from part of the trap is maximum.
Mathematically, we can write the maximum of $S(T; t_1, t_2)$ as:

$$\frac{dS}{dT} = \frac{dS}{de_n}\frac{de_n}{dT} = 0$$

By considering the equation of the current transient in an electric field and the equation of the emission probability rate, the solution brings to:

$$e_n(t_1 - t_2) = \ln\frac{(1-e_n t_2)}{(1-e_n t_1)}$$

This is a transcendental equation so it must be solved numerically via software analysis that tells us what is the value of the thermal emission rate e_n we are scanning, given t_1 and t_2.
By changing values of t_1 and t_2, that is, by changing rate window, we obtain a curve $S'(T; t'_1, t'_2)$ identical to the previous one but shifted, since now the value of e_n and T_m differ from the previous one. Therefore, by choosing a collection of values t_1 and t_2 it is possible to obtain a collection of values e_n as a function of T_m. By recalling the link between e_n and T, we can obtain an Arrhenius plot of the form:

$$\ln\left(\frac{T_m^2}{e_m(T_m)}\right) = \gamma\sigma + \frac{E_a}{K_b T_m}$$

Then, in order to deal with problems related to a temperature dependence into the sensitivity of the system of so similar peak heights at different temperatures, the PICTS signal is normalized to the magnitude of the photocurrent during the illumination period.

A real example of what has just explained is shown in *Figure 7* , where a set of current transient is plotted as a function of temperature:

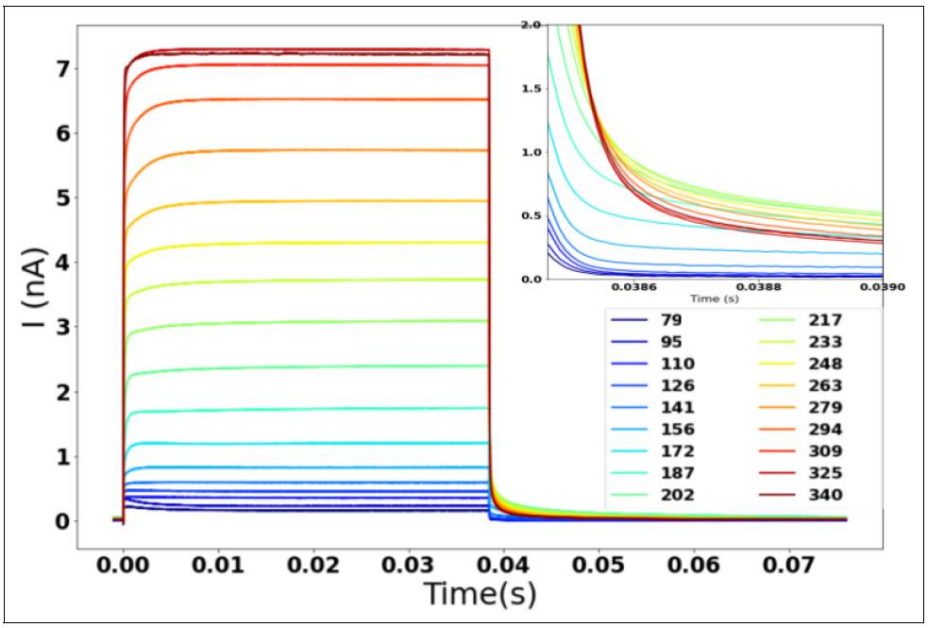

Figure 7 Schematic representation of a set of current transients as a function of the temperatures, from 79K (blue line in the box) to 340K (brown line in the box)

The signal consists of what appears to be several shifted copies of the same curve at different rate window values, which is expressed in Hertz and coincides with the value of $(t_1–t_2)^{-1}$, where each pair is represented by the same colour. In the example shown, there is a maximum between 150K and 200K, that coincide with a maximum shift of the transient decay. The transients collected are then rearranged and analysed in order to obtain the PICTS spectrum as shown in *Figure 8 a)*. The shape of the PICTS spectrum around the maximum is not predictable by the theory, therefore the identification of the maximums is obtained through a Gaussian fit that take the advantage of a function optimization algorithm (i.e. find the maxima through the derivatives) that not lends itself to being a variable choice and does not introduce artifacts in the graph. What comes next is an Arrhenius plot: the curves are fitted in the maximum zone to obtain, for each peak, a pair of values (e_n, T_m) (see *Figure 8b*). These points are then inserted in a semilogarithmic graph where they appear as straight lines. Through the slope it is thus possible to obtain the value of the activation

energy and from the intercept the capture cross section. Going a step further, it is also possible to better observe the traps. If instead of generating a handful of rate windows we proceed generating a large number of them, it is possible to obtain a two-dimensional map of $\ln(e_n)$ as a function of the temperature. This process is shown in *Figure 8 c),* where the trap is now clearly seen. These graph, called map, are very useful for qualitatively comparing the shape of deep levels in samples.

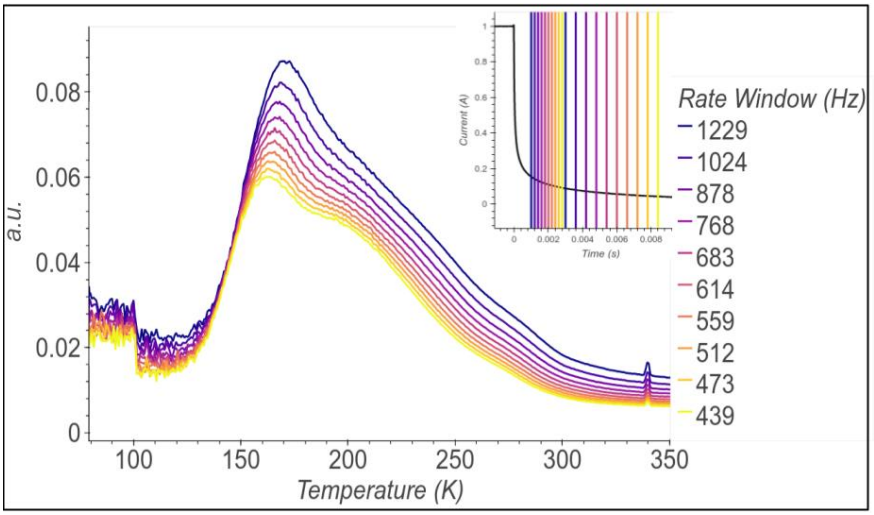

(a)

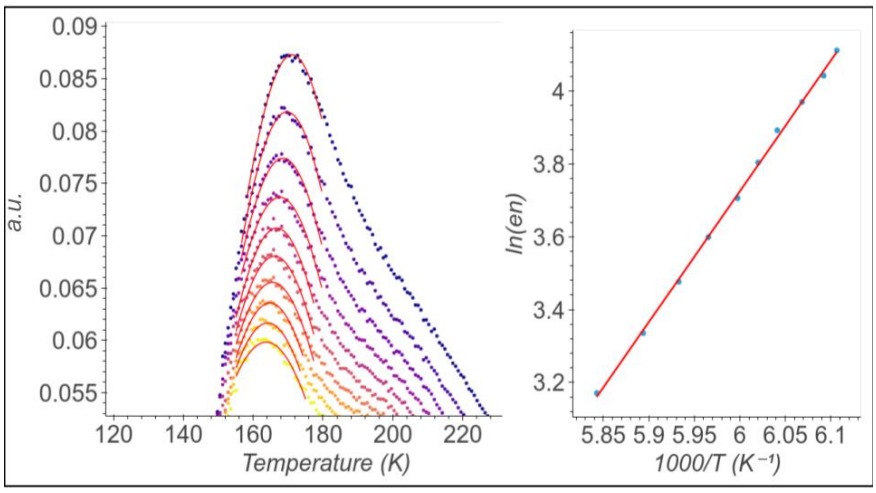

(b)

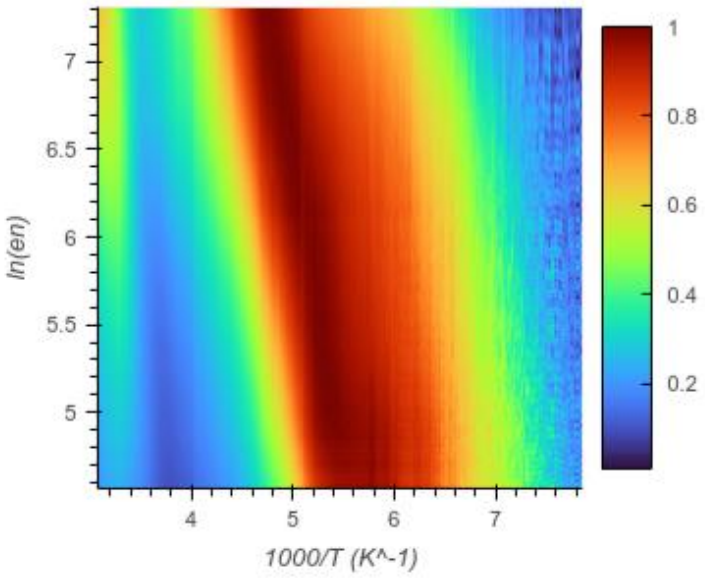

(c)

Figure 8 a) PICTS spectrum for several rate window; b): Detail of the above PICTS spectrum with the Arrhenius plot; c) Another way to view a PICTS spectrum: a map

3. Results and Discussion

3.1. I/V characteristic with probe station and fitting

Many information can be extracted from a current-voltage characteristic (namely *I-V diagram*). What is of interest are mostly three things:

- verify that the sample inserted in its sample holder and the including contacts of it has an ohmic behaviour;
- verify if ionic currents are present, possibly measuring the ionic activation energies of those;
- calculate the Resistivity and Responsivity of the samples.

In the first case the speech is extremely simple: material is said to be ohmic when the ratio between the current flowing inside the sample and the potential difference remains constant. This quantity is called conductance and in *Figure 9* are shown two typical behaviours that usually occur in nature: that of metals, purely ohmic, and that of Schottky or pn junctions, also called "Rectifying".

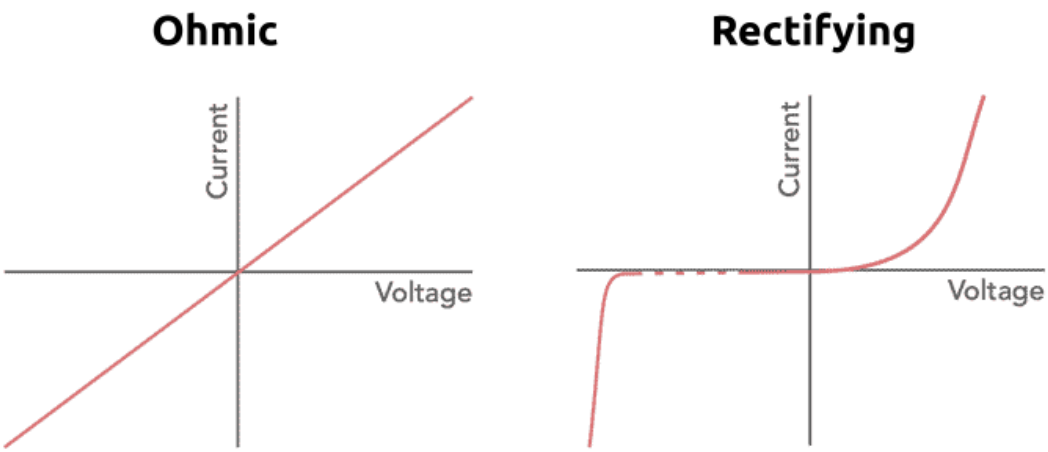

Figure 9 Two common types of behaviour for I-V diagram: purely Ohmic (left) as for a metal, and the rectifying one (right) of Schottky or pn junctions.

The typical physical quantity of reference in these cases is not the conductance itself, which also depends on geometric factors, but the electrical conductivity, which instead is an intrinsic quantity of the material and it is usually a function of temperature. A link can be found between electrical conductivity and the activation energy of ion currents within a material.
In this way, by measuring the electrical resistance of the sample as the temperature varies and plotting the related Arrhenius plot, it is possible to experimentally access, if they exist, the ion activation energy values.
One of the purpose of this thesis work, also, is to determine the Resistance, the Responsivity, the External Quantum Efficiency (EQE) and the Detectivity of the sample through I-V characteristics, in dark and under UV light, in order to compare these values with the ones at the time when the samples has been fabricated. Thus, we can achieve a direct information of how the samples degrade through the years (see par. 1.2.1). In fact, by plotting Voltage vs. Current values it is directly possible to obtain resistance R, by using Ohm's Law:

$$V = RI \rightarrow R = \frac{V}{I}$$

To achieve this result a probe station capable of measuring ultra low-current (fA) has been used, as shown in *Figure10*:

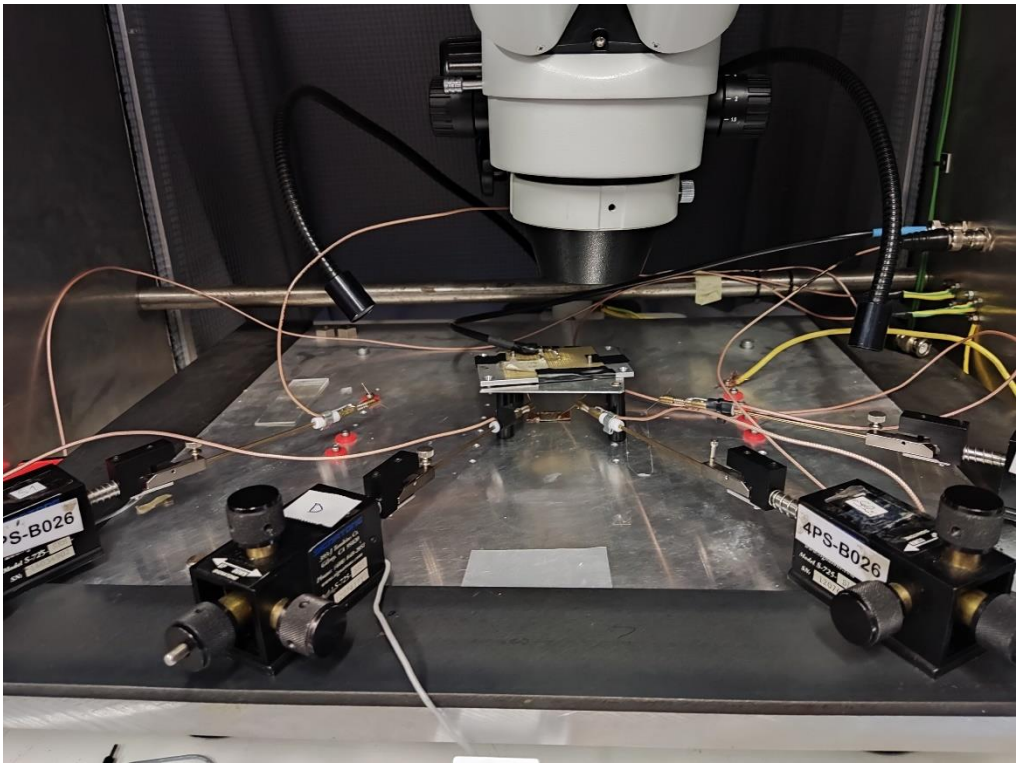

(a)

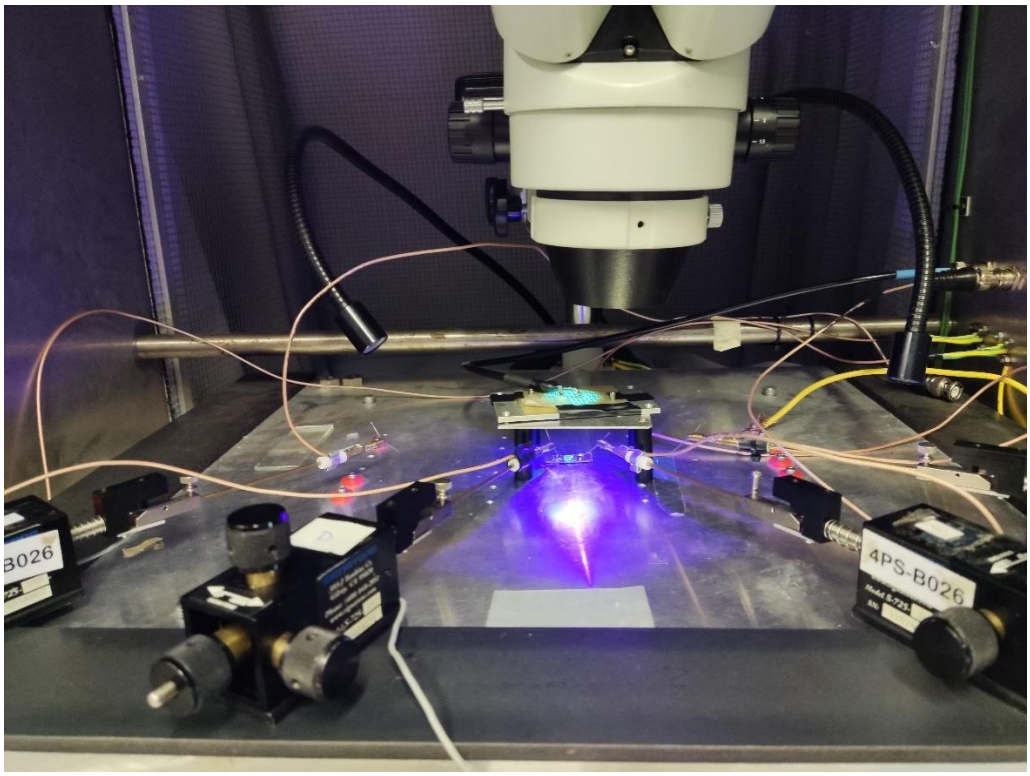

(b)

Figure 10 Probe station used to determine I-V characteristic when: a) led is off and b) led is on

Two probes are respectively connected with the positive and negative poles of the samples. Then the measure of I-V characteristic is taken in two steps: first when the led is off and then

with the led on, for the purpose of measuring the Responsivity of each sample.
In *Figure12* the three I-V diagrams are reported:

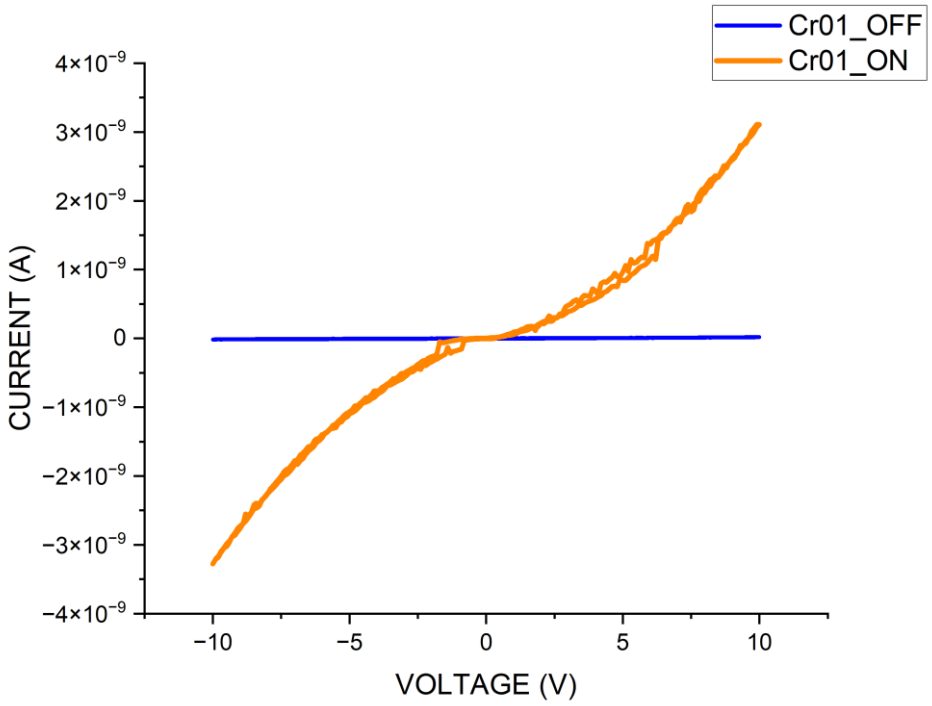

(a)

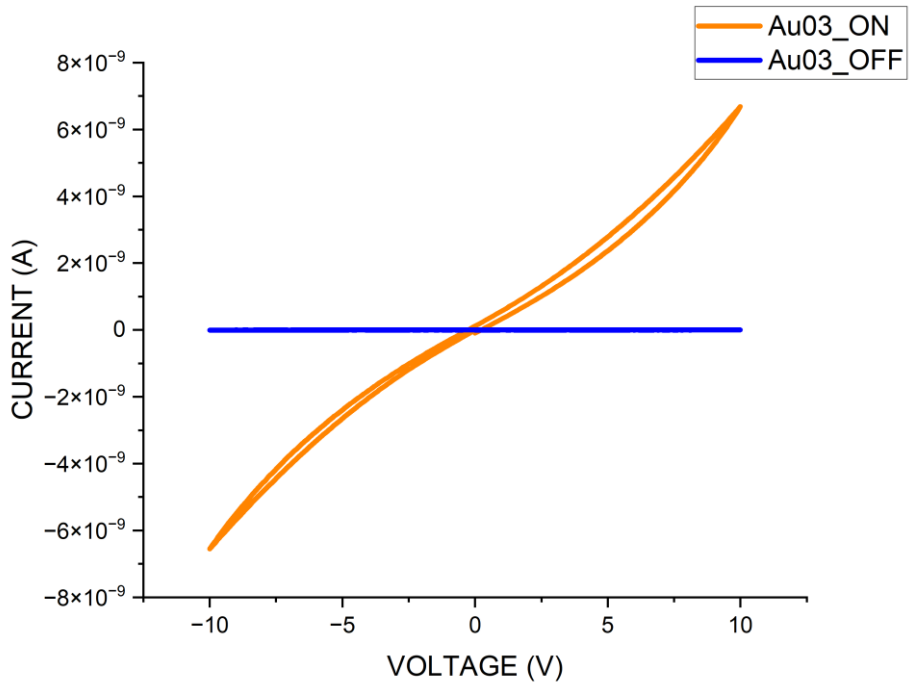

(b)

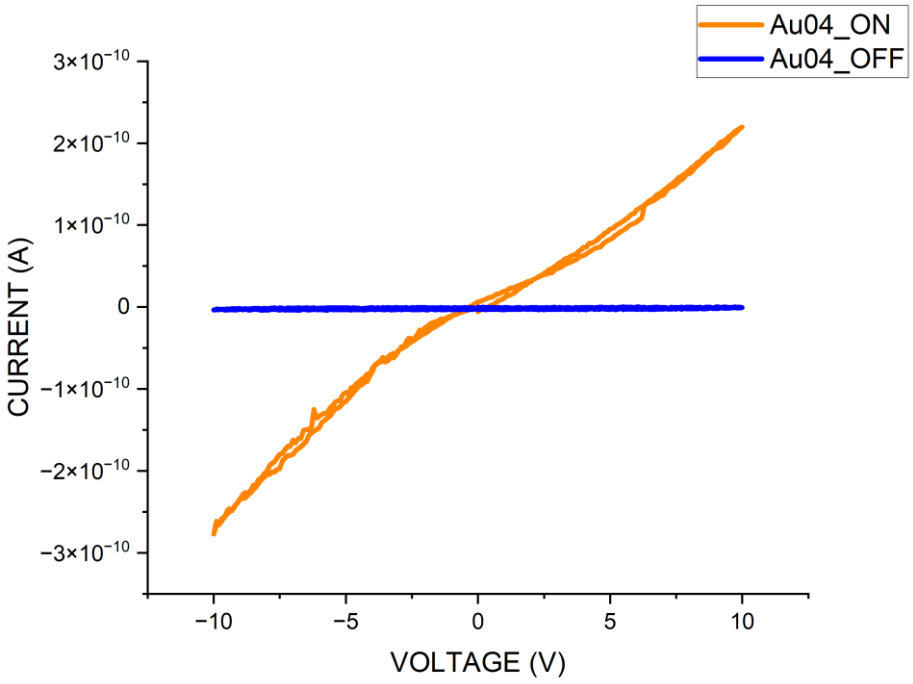

(c)

Figure 11 2024 I-V characteristic of: a) Cr01, b) Au03, c) Au04 samples

To characterize the sample and so to calculate *R*, the only I-V necessary is the one at "*dark condition*", that means when the led is off: by making a linear fit of this curve we obtain the conductance *G*. Because Conductance and Resistance are reciprocal, through the value of "*slope*" obtained by the fitting we can easily calculate *R* as:

$$R = \frac{1}{G} = \frac{1}{"slope"} = \frac{V}{I}$$

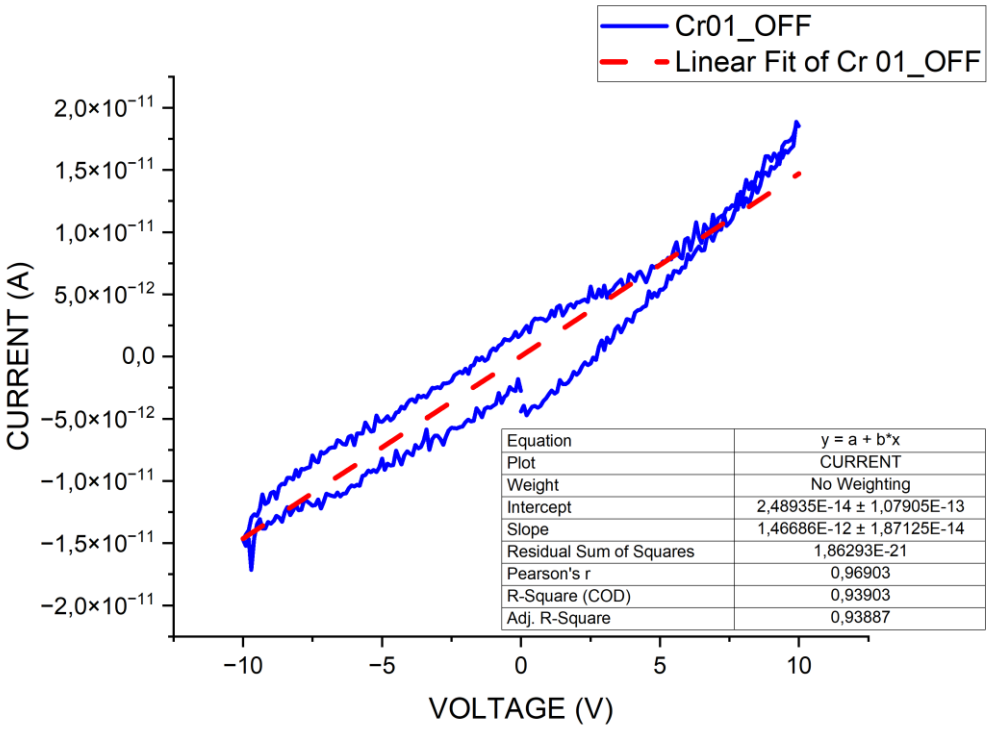

Equation	y = a + b*x
Plot	CURRENT
Weight	No Weighting
Intercept	2,48935E-14 ± 1,07905E-13
Slope	1,46686E-12 ± 1,87125E-14
Residual Sum of Squares	1,86293E-21
Pearson's r	0,96903
R-Square (COD)	0,93903
Adj. R-Square	0,93887

(a)

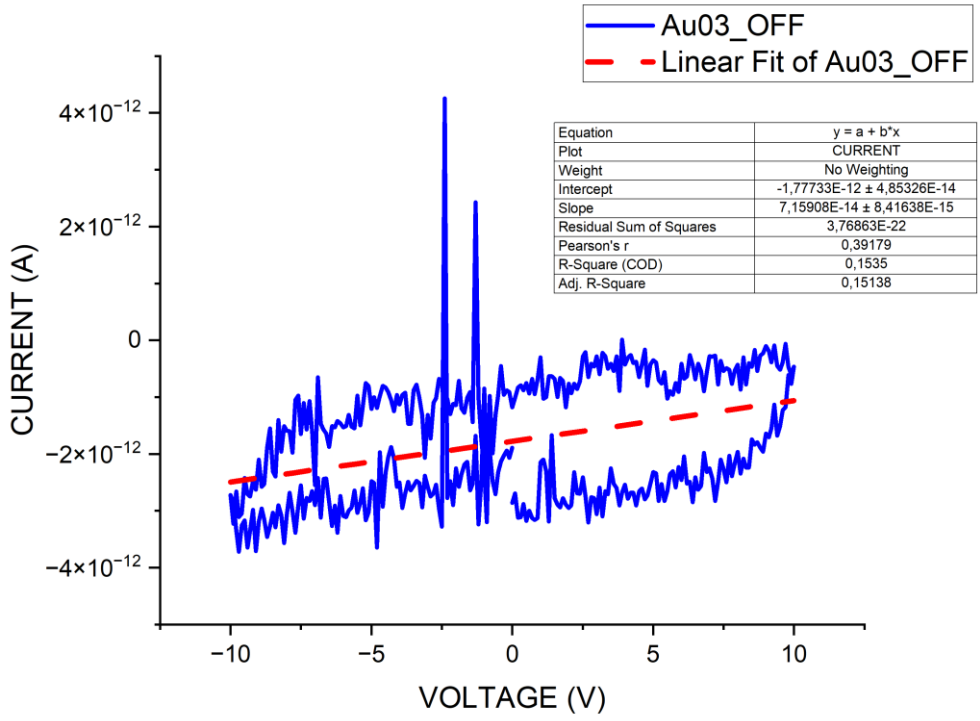

Equation	y = a + b*x
Plot	CURRENT
Weight	No Weighting
Intercept	-1,77733E-12 ± 4,85326E-14
Slope	7,15908E-14 ± 8,41638E-15
Residual Sum of Squares	3,76863E-22
Pearson's r	0,39179
R-Square (COD)	0,1535
Adj. R-Square	0,15138

(b)

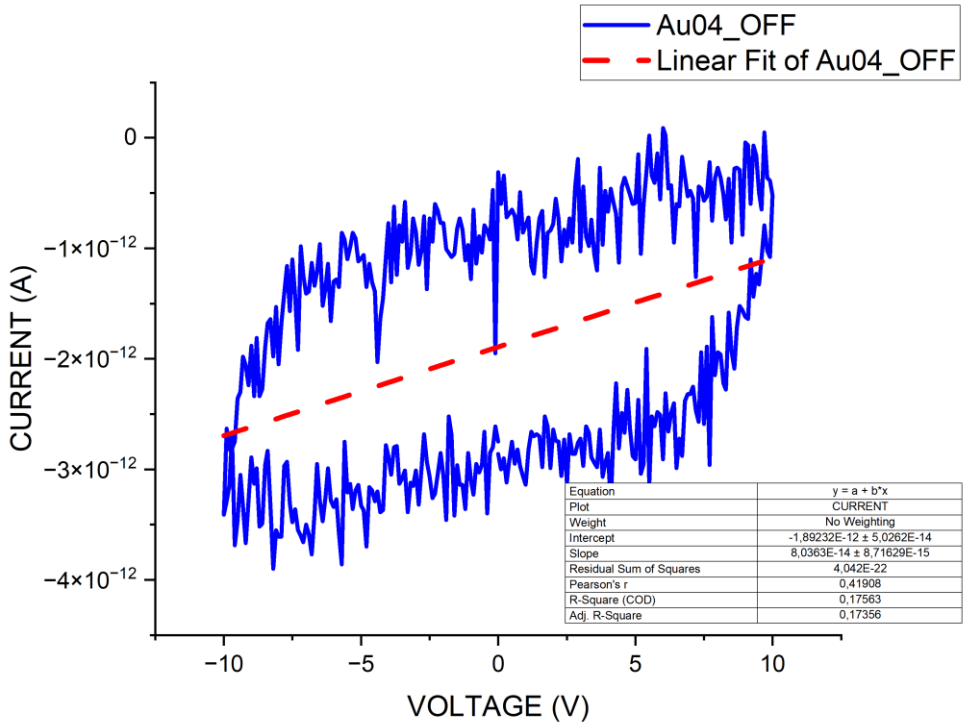

(c)

Figure 12 2024 I-V diagrams of OFF phase and fitting of the three sample: a)Cr01, b)Au03, c)Au04

The curves from I-V diagrams in *Figure12* are not straight lines but they show a hysteresis trend because of the capacitive transients that occur in the samples during acquisitions. In order to minimize these effects, the time acquisition between two consecutive values of Voltage have been reduces: in this way the capacitive transients can drop slowly and the hysteresis trend tend to a straight line.
In this way it is clear that the samples verify the ohmic trend, as expected.

We extracted the same parameters from the I-V taken in 2022 (as-grown samples) and we compare them with the I-V in 2024. The values we got are summarise in *Table 1*:

	2022	
	G [Ω^{-1}]	**R** [Ω]
Cr01	(6.7 ± 0.7) x10^{-12}	(1.5 ± 0.2) x10^{11}
Au03	(1.72 ± 0.02) x10^{-12}	(5.81 ± 0.06) x10^{11}
Au04	(6 ± 1) x10^{-14}	(1.73 ± 0.30) x10^{13}

	2024	
	G [Ω^{-1}]	**R** [Ω]
Cr01	(1.47 ± 0.02) x10^{-12}	(6.82 ± 0.09) x10^{11}
Au03	(7.2 ± 0.8) x10^{-14}	(1.40 ± 0.2) x10^{13}
Au04	(8.04 ±) x10^{-14}	(1.3 ± 0.1) x10^{13}

Table 2 Values of Conductance and Resistance of the three samples in 2022 and 2024

What arise from the *Table 2* is that the more the defects increase in the detectors, the more does the Resistance and, consequently, the mobility of the charges decrease, being the electrical resistance of an object a measure of its opposition to the flow of electric current. The dark current is dominated by the transport free charges and their movements is hindered by the defects.

On the other hand, comparing the values of R in 2022 and 2024 seems that Cr01 and Au04 are pretty stable, keeping the same magnitude of R, while sample Au03 shows a bigger increase in R, of 2 order of magnitudes from (5.81±0.06)x10 ^{11} Ω to (1.4±0.2)x10 ^{13} Ω.

3.2 Responsivity, EQE and Detectivity as characterization parameters for detectors

When it comes to photodetectors, evaluating their performance is crucial to determine their operation. Several key parameters are considered to be figures of merit in these detectors, and knowing these parameters is essential for a proper evaluation of a device's performance.

These performance parameters include but are not limited to: Responsivity, External Quantum Efficiency (EQE) and Detectivity, that will be explained hereafter. Understanding these parameters and their interplay is crucial for designing and develop their properties. Knowledge of the Responsivity, EQE and Detectivity, in fact, allow the user to determine how much detector signal will be available for a specific application.

Responsivity, is defined as the output signal of a detector produced

in response to a given incident radiant power falling on the detector itself [10]. The units of responsivity are either Amperes/Watt or Volts/Watt, depending on whether the output is an electric current or a voltage. However, Responsivity can be express by the following equation:

$$Responsivity = \frac{\Delta I_{pc}}{p_0 A}$$

where $\Delta I_{pc} = I_{on} - I_{off}$ is the difference of the photocurrent when the led is respectively on and off, p_0 represents the intensity of the incident light of the led, taken from led I-V calibration diagram and A is the active sensor area where the led hits the sample surface. For our set-up and samples, the following parameters have been used:

p_0 =0,116 mW/mm^2

$A \approx 1.3\ mm^2$

Doing so, what we obtain is shown in the *Figure13*:

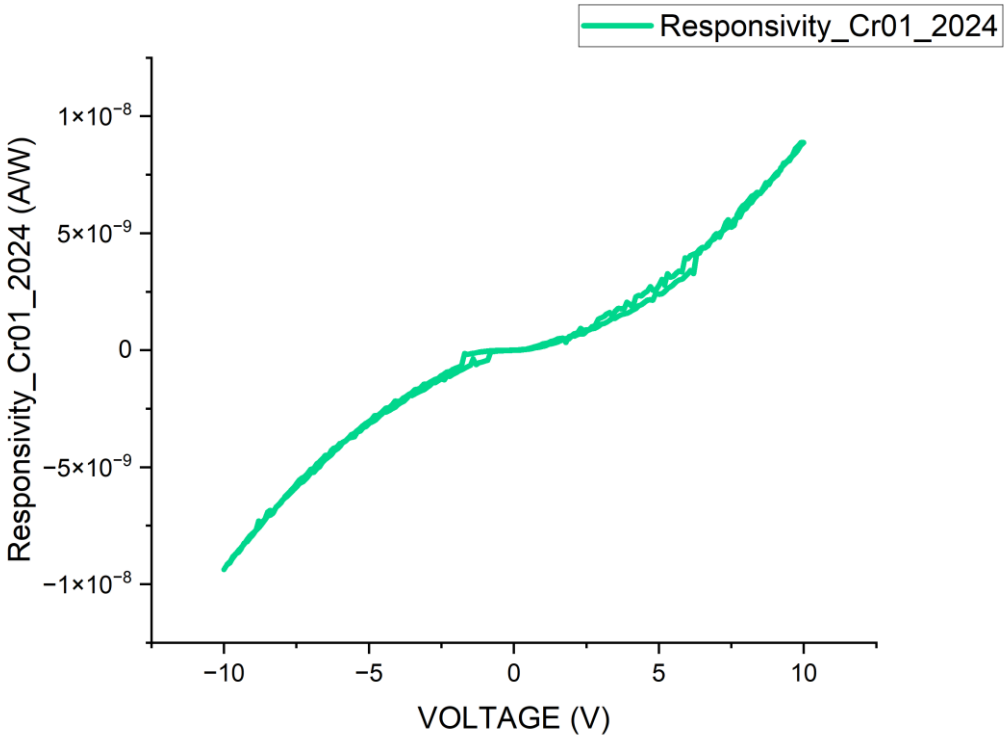

(a)

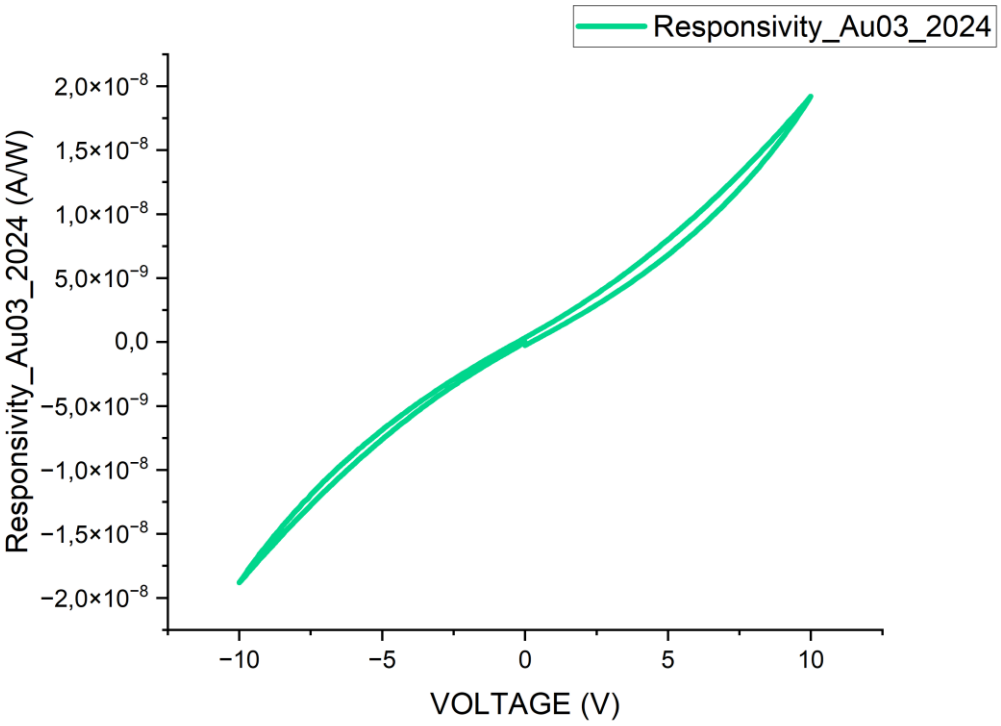

(b)

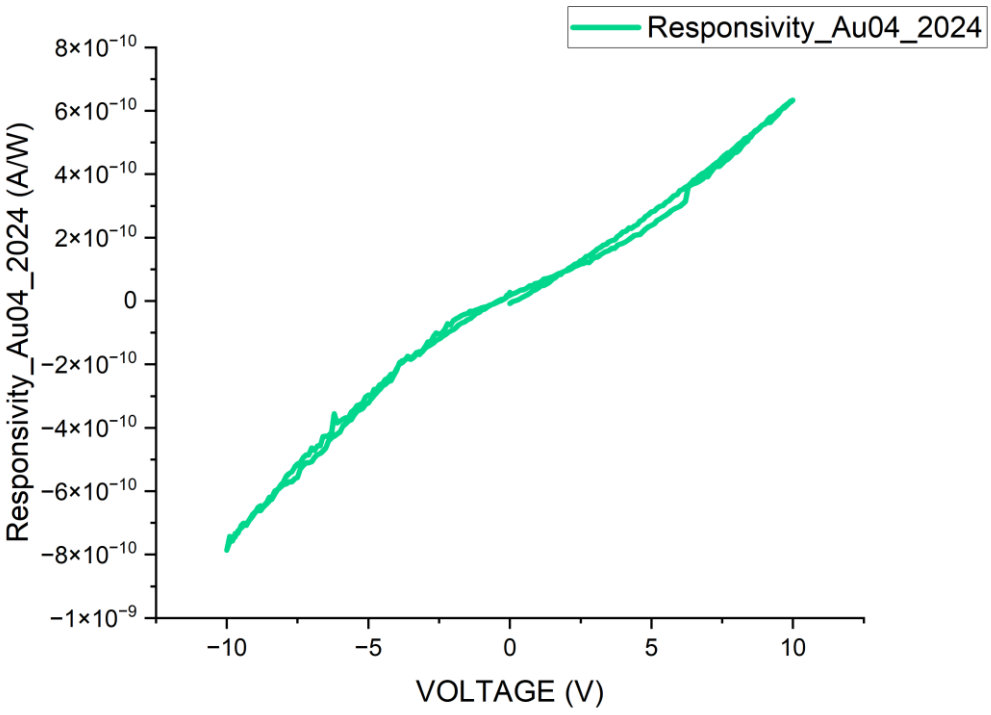

(c)

Figure 13 Responsivity of: a)Cr01, b)Au03 and c)Au04, in 2024.

External Quantum Efficiency (EQE) is the ratio of the number of carriers (N_e) collected by the electrodes of the photodetector to the number of incident photons (N_{ph}) on its surface. If V is the applied biasing voltage and R is the resistance across which the signal has to be detected, the external quantum efficiency can be also defined as the ratio of carrier flux ($\emptyset_c$) to that of photon flux ($\emptyset_{ph}$) [11]:

$$\eta = \frac{\emptyset_c}{\emptyset_{ph}} = \frac{\frac{I_p}{q}q}{\frac{P_{opt}}{\mathrm{hv}}}$$

where I_p is photogenerated current and it is equal to the difference of current generated, and q is a charge on carriers, P_{opt} is the optical power incident, h is Plank constant, υ is the frequency of the incident photon. The quantum efficiency is basically another way of expressing the effectiveness of the incident optical energy for producing an output of electrical current. The quantum efficiency Q in percent [%] may be related to the Responsivity by the equation:

$$Q = 100 * R * \frac{1.2395}{\lambda}$$

where R is the Responsivity (in amperes per watt) of the detector at wavelength λ (in micrometers).

The *Detectivity* D of a photodetector is a figure of merit, defined as the inverse of the noise-equivalent power (NEP), which is the optical input power that produces an additional output identical to that noise power for a given bandwidth. The larger the detectivity of a photodetector, the more it is suitable for detecting weak signals which compete with the detector noise [12].

Depending on the purpose, it is more useful to define the *Specific detectivity* $D*$, which is the detectivity normalized to a unit detector area (1 m^2) and detection bandwidth (1 Hz), expressed as:

$$D* = \sqrt{\frac{A*Responsivity^2}{2q*I_{10V}}}$$

where A is the area of the detector, q is the charge of the electron and I_{10V} is the value of the current at 10 Voltage. The unit of

Detectivity is 1/W, while Specific detectivity has the unit of $cm*Hz^{1/2}/W$, also known as Jones unit.

Expressed in this way, Specific detectivity is helpful for comparing the performance of different detector technologies. If the detector bandwidth scales inversely with the active area, typically because of the limiting impact of the electrical capacitance, the specific detectivity will be independent from the active area.

In contrast to the Responsivity, the Detectivity is influenced by detector noise. Improving the Responsivity improves the Detectivity only if the noise level is increased less than the signal level.

To sum up those properties of the samples, taken in 2022 and 2024, we get:

	2022			
	ΔI_{pc} (10V) [A]	**Responsivity (10V)** [A/W]	**EQE** [%]	**Specific Detectivity** [Jones]
Cr01	2.44×10^{-9}	7.01×10^{-9}	23	1.77×10^{3}
Au03	7.32×10^{-9}	2.10×10^{-8}	68	1.89×10^{4}
Au04	1.59×10^{-8}	4.57×10^{-8}	147	3.60×10^{5}

	2024			
	ΔI_{pc} (10V) [A]	**Responsivity (10V)** [A/W]	**EQE** [%]	**Specific Detectivity** [Jones]
Cr01	3.05×10^{-9}	8.78×10^{-9}	28	6.19×10^{3}
Au03	6.56×10^{-9}	1.89×10^{-8}	61	7.00×10^{2}
Au04	2.20×10^{-10}	6.33×10^{-10}	2	1.30×10^{2}

Table 3 Delta photocurrent, Responsivity, EQE and Detectivity of the three samples in 2022 and 2024 with an estimation of the error of at least 5%

The values of Resistance analysed in par.3.1*, Table 2* show that the current is due to the mobility of the charges; from *Table 3* we can notice that the samples with more defective structure, even if they show less mobility of the charges (higher Resistance values), exhibit a higher

Responsivity with respect to defect-free sample Cr01. This means that the photoconductive process is due to defects, typically associated to a photoconductive gain process, that result in EQE values higher than 100%.

Responsivity values of 2022 show that materials with defects are more likely to give a strong electrical signal when an incident photons from the led hits their surface, since Responsivity increase from pure Cr01 to Au03 and Au04 samples of one order of magnitude. Interestingly, the Responsivity decreases with time (if compared with values from 2024), as more defects are present in the material: Responsivity of Au04 decreases from $4.57x10^{-8}$ A/W in 2022 to $6.33x10^{-10}$ A/W in 2024, up to 2% of its initial value. This is confirmed by EQE values, being EQE directly related to Responsivity unless a constant value determined by the wavelength of the led source. EQE as a percentage value represent the amount of charges collected respect to the incident photons and from the *Table 2* it's easy to figure out how this value increase a lot during the formation time of the samples in 2022 from 23% of pure Cr01 up to 147% of high defective Au04, but it also degrade a lot across the years the more the defect increase in the material: it results almost stable for Cr01 and Au03, but in Au04 since it decrease its Responsivity of 18% in two years, EQE collapse from 147% in 2022 to only 2% in 2024.

Finally, Specific detectivity has been analyse, remembering that a high value of D* means that the detector is suitable for detecting weak signals in presence of noise. From what arise from the *Table2*, again, detector with many defects seems to be more suitable for the purpose when made but they show a high degradation over a long period of time: in fact Cr01 remains almost constant over the years, Au03 decrease of two order of magnitudes, from $1.89x10^{4}$ Jones in 2022 to $7.00x10^{2}$ Jones in 2024, while specific detectivity of Au04 goes from $3.60x10^{5}$ Jones in 2022, to $1.30x10^{2}$ Jones in 2024, showing a decrease of even three order of magnitude.

3.3 PICTS analysis

In order to achieve a better understanding of the sample under analysis and to characterize the defects in the samples after two years, a PICTS experiment has been performed. First, we acquire the transients at different temperatures steps, from 87K up to 350K. In *Figure 14* is shown a transient from Cr01 sample at 248.85K.

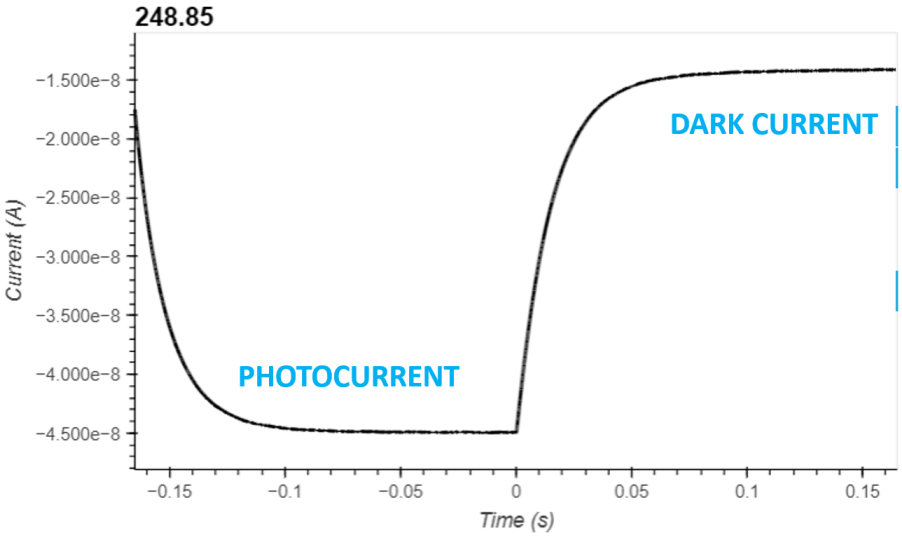

Figure 14 Transient of Cr01 sample at 24.5K

The transient has an inverse behaviour due to the polarity of the connection that does not influence the data analysis. In the next step, in fact, the transient has been swapped and normalized, as shown in Figure 15:

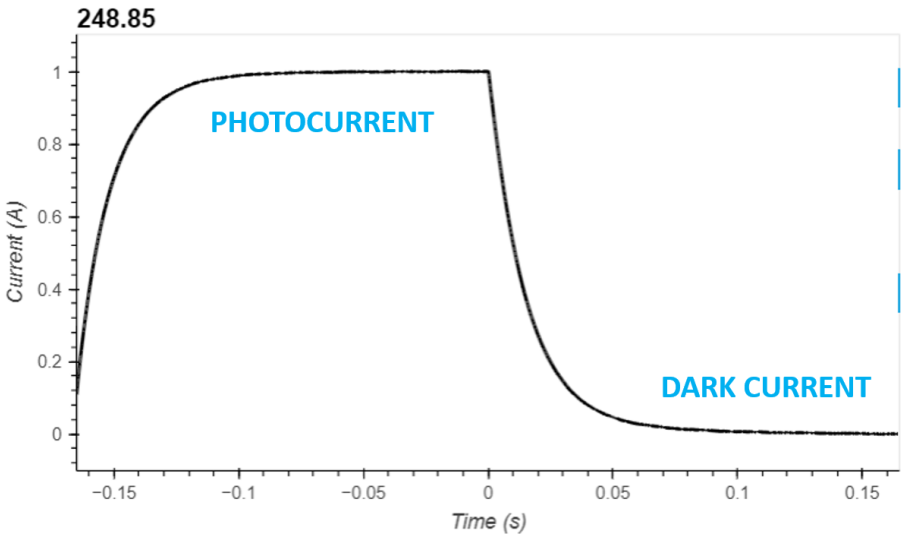

Figure 15 Normalized transient of Cr01 sample at 248.85K

Onto the data collected every 0.5 K, we carried out Double Gate Analysis (see par. 2.2.1), and we calculated a map of the logarithm of the emission rate as a function of the inverse of the temperature, as shown in *Figure 16:*

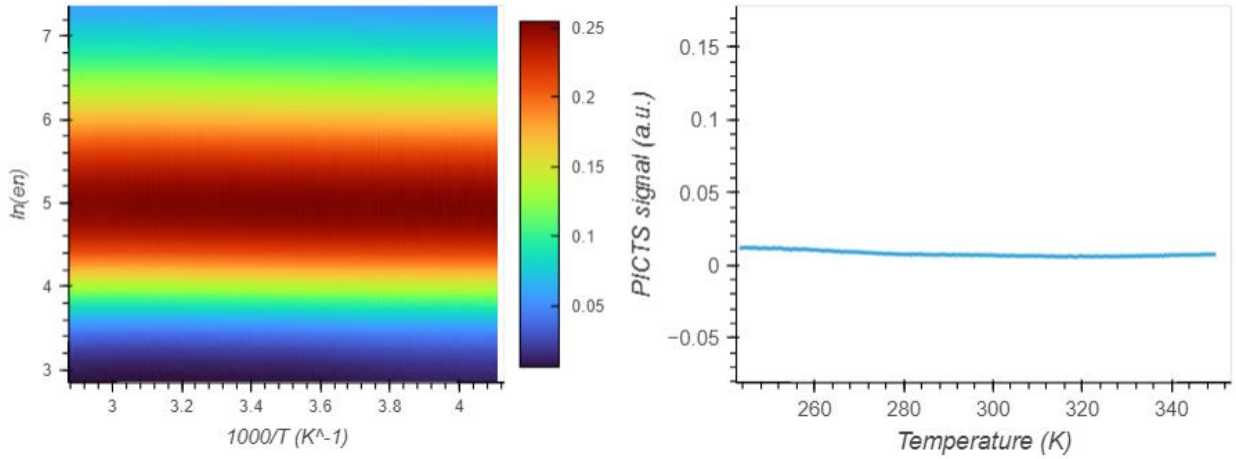

Figure 16 PICTS map of Cr01 sample

From the colormap of Figure 16 (left) no significant peaks has been detected: the area coloured in red show that there is no changes in the emission rate while temperature increase. This result is in contrast with the same experiment performed in 2022 on the same sample and shown in *Figure 17* highlight the presence of three defects in the material.

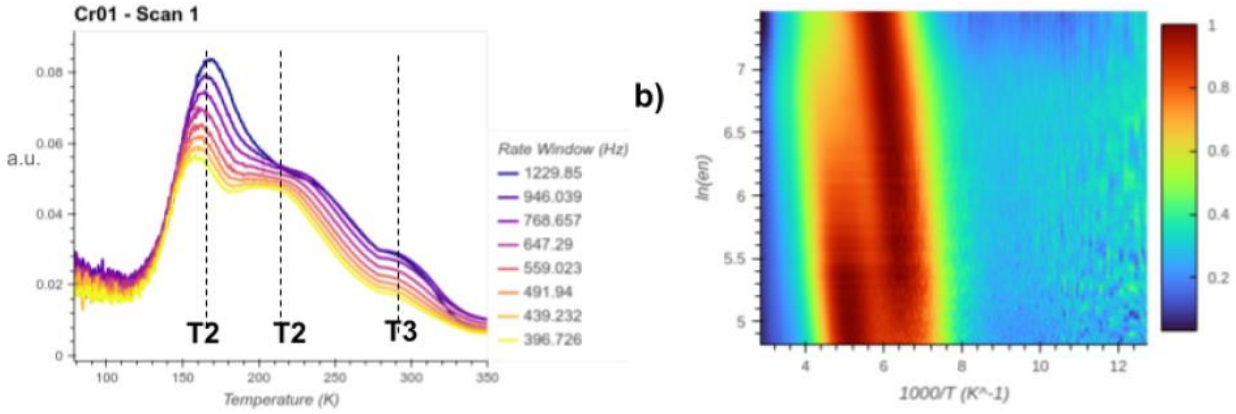

Figure 17 PICTS signial profile (left) and PICTS map (right) of Cr01 in 2022. Taken from [14]

The reason for our recent result in 2024 is still under investigation (e.g. lack of sensitivity of the experimental apparatus or strongly

reduction in the spatial density of the defect states) and thus we do not mention it in the conclusions.

4. Conclusions

Despite the excellent opto-electronic properties shown in the analysis of the samples at the time of their fabrication, Perovskites have the big problem of degrading within a few years or less, if not encapsulated and protected from the external environment.
Analysing their characteristic properties of Resistance, Responsivity, EQE and Detectivity arise a good behaviour as detector as- grown but also show a fast degradation across the years.
In this thesis work the incidence of defects has been taken into account to see how they affect the properties of the material and weigh on the selection of a particular detector for specific applications. For this purpose the three sample studied were, respectively made as: defect-free Cr01, 1 molar defective Au03 and 10 molar defective Au04.
Looking at their properties and how they change trough years seems that pure Chromium sample is the most stable among them: it slightly increase its Resistance and Responsivity from its initial values, keeping the same order of magnitude for both.
Au03 sample, instead, increase a lot its Resistance, from $(5.81\pm0.06)\times10^{13}\Omega$ in 2022 to $(1.40\pm0.20)\times10^{11}\Omega$ in 2024, while keeping its Responsivity almost on the same order of magnitude.
This result suggests that the photo response of detector improve in presence of defects, being Au03 1 molar defective sample. On the other hand, Au04 sample sees its Responsivity collapsing drastically trough years, decreasing this value of two orders of magnitude: from this result we can suppose that there is a limit of defects in the material for which the opto-electronic properties improve, and beyond which these properties collapse drastically.
Actually, this is an assumption that deserve to be studied much more in details. Looking at the samples under the microscope, in fact, it's clear that those are degraded a lot, especially Au04 sample, as shown in *Figure 1,* confirming that the way how perovskites are stored and protected from external environment influence a lot their properties and the degradation of material.

Bibliography

[1] Yvonne J Hofstetter, Ines Garcia-Benito, Fabian Paulus, Simonetta Orlandi, Giulia Grancini, and Yana Vaynzof. “Vacuum-induced degradation of 2D perovskites.” In: Frontiers in chemistry 8 (2020), p. 66.

[2] Carter W. Craig Balluffi Robert W Allen Samuel M. Kinetics of Materials. vol. 10.1002/0471749311. John Wiley & Sons, Inc., 2005 September 23.

[3] Erik Gregersen, Gloria Lotha, Grace Young. “Activation energy”. In: The Editors of Encyclopaedia Britannica.

[4] WTRW Shockley and WT Read Jr. “Statistics of the recombinations of holes and electrons.” In: Physical review 87.5 (1952), p. 835.

[5] Re N Hall. “Electron-hole recombination in germanium.” In: Physical review 87.2 (1952), p. 387.

[6] Christie LC Ellis, Emily Smith, Hamza Javaid, Gabrielle Berns, and Dhandapani Venkataraman. “Ion migration in hybrid perovskites: Evolving understanding of a dynamic phenomenon.” In: Perovskite Photovoltaics (2018), pp. 163–196.

[7] Christie LC Ellis, Emily Smith, Hamza Javaid, Gabrielle Berns, and Dhandapani Venkataraman. “Ion migration in hybrid perovskites: Evolving understanding of a dynamic phenomenon.” In: Perovskite Photovoltaics (2018), pp. 163–196.

[8] Yunxia Zhang, Yucheng Liu, Zhuo Xu, Haochen Ye, Qingxian Li, Mingxin Hu, Zhou Yang, and Shengzhong Frank Liu. “Twodimensional $(PEA)_2PbBr_4$ perovskite single crystals for a high performance UV-detector.” In: Journal of Materials Chemistry C 7.6 (2019), pp. 1584–1591.

[9] J. W. Orton P. Blood. The Electrical Characterization of Semiconductors: Majority Carriers and Electron States. Academic Pr., 1992. isbn: 0125286279; 9780125286275.

[10] Pallab Bhattacharya, Roberto Fornari and Hiroshi Kamimura, Comprehensive Semiconductor Science and Technology 2011. isbn: 978-0-444-53153-7.

[11]Nasir Ali, Sanam Attique, Arash RahimiI, Shahid Ali, Fazli Akram, Ning Dai, Huizhen Wu. “Beyond lead: Progress in stable and non-toxic lower-dimensional perovskites for high-performance photodetection”. Sustainable Materials and Technologies Volume 38, December 2023

[12] Dr. Rüdiger Paschotta, https://doi.org/10.61835/shj

[13] Dongguen Shin, Fengshuo Zu, Edgar R. Nandayapa, Lennart Frohloff, Emily Albert,Emil J. W. List-Kratochvil, and Norbert Koch. “The Electronic Properties of a 2D Ruddlesden-Popper Perovskite and its Energy Level Alignment with a 3D Perovskite Enable Interfacial Energy Transfer”. In: Advanced Functional Materials, 2023, n° 33.

[14] Vito Foderà. “Characterization of in-gap Electronic States in Two-Dimensional Single Crystal PEA2PbBr4 Perovskite for X-ray Detection”, Master Degree Thesis, A.A. 2021/2022

[15] Ferdinand Lédée, Andrea Ciavatti, Matteo Verdi, Laura Basiricò, and Beatrice Fraboni. “Ultra-Stable and Robust Response to X-Rays in 2D Layered Perovskite Micro-Crystalline Films Directly Deposited on Flexible Substrate”. In: Advanced Functional Materials, 2021.

[16] Giovanni Armaroli, Lorenzo Maserati, Andrea Ciavatti, Pierpaolo Vecchi, Alberto Piccioni, Martina Foschi, Valentina Van der Meer, Chiara Cortese, Matias Feldman, Vito Foderà, Thibault Lemercier, Julien Zaccaro, Javier Mayén Guillén, Eric Gros-Daillon, Beatrice Fraboni, and Daniela Cavalcoli. In: “Photoinduced Current Transient Spectroscopy on Metal Halide Perovskites: Electron Trapping and Ion Drift”. In: ACS Energy Lett. 2023, 8, 4371−4379.